The 6th TSME International Conference on Mechanical Engineering
16-18 December 2015

TSF006

Effects of the Azimuthal Positions of the Azimuthal Control Jets on Structures and Entrainment of a Jet in Crossflow at High Effective Velocity Ratio 12

Saran Wangkiat, Sumate Khemakanon, Apichote Kengkarnpanich, and Asi Bunyajitradulya*

Department of Mechanical Engineering, Faculty of Engineering, Chulalongkorn University, Bangkok 10330, Thailand
* Corresponding Author: E-mail: asi.b@chula.ac.th, Tel: 02 218 6645, Fax: 02 218 6645*

Abstract

The effects of azimuthal positions θ of azimuthal control jets on the structure and entrainment of a jet in crossflow (JICF) at a moderately high effective velocity ratio r of 12 are investigated. This research is our continuing effort in finding an effective means for manipulating and controlling entrainment of a jet in crossflow as well as evaluating the use of the azimuthal control jets in this regard. In this respect, we have reported the application of the azimuthal control jets to a JICF at low effective velocity ratio r of 4 in the past (Witayaprapakorn and Bunyajitradulya [1], Witayaprapakorn [2], and Chaikasetsin *et al*. [3]). This research attempts to further investigate whether the azimuthal control jets can be as effective in manipulating and controlling entrainment of a JICF at higher effective velocity ratio. On related aspect, in order 1) to be able to instantaneously and clearly identify and differentiate the jet-fluid mixture region and structures from the surrounding pure crossflow region, and consequently 2) to be able to determine the accumulative volumetric entrainment ratio E of a jet more accurately, a Stereoscopic Particle Image Velocimetry (SPIV), in which only the main jet fluid – and not the crossflow fluid – is seeded with PIV tracer particles, is used. As a result, the SPIV instantaneously registers only velocity vectors from the jet-fluid mixture region (i.e., the region with some main jet fluid as marked by some PIV tracer particles) and registers none from the surrounding pure crossflow region (i.e., the region with no main jet fluid as marked by no PIV tracer particles). Consequently, the instantaneous and, subsequently, the time-mean jet-fluid mixture volume flowrate and jet volumetric entrainment ratio can be determined. Furthermore, the present technique of using SPIV together with the jet-fluid only seeding scheme does not only allow us to determine the entrainment ratio more accurately but also gives us information on the probability of finding jet-fluid mixture at a point, the jet probability structure, and the related probabilistic characteristics of turbulent jet. For the cases of controlled jets in crossflow (cJICF), a pair of azimuthal control jets is injected radially and steadily at the azimuthal positions (θ) of $\pm 15^\circ$, $\pm 45^\circ$, $\pm 75^\circ$, $\pm 105^\circ$, $\pm 135^\circ$, and $\pm 165^\circ$, hereafter referred to as case Iθ, at the total azimuthal control jets to main jet mass flowrate ratio (r_m) of 4%. The results show that the azimuthal control jets position θ affects the jet probability, velocity, and vorticity structures to various degree depending upon θ. Windward injection ($\theta < 90^o$) typically modifies the jet structures considerably; lowers the jet trajectories; and suppresses entrainment, making the effectiveness less than one, when compared to JICF. On the other hand, leeward injection typically results in the opposites. Namely, it modifies the jet structures relatively less – except for the appearance of the wake-like structure at the underside of the jet; raises the jet trajectories (except case I165); and promotes entrainment, making the effectiveness more than one, when compared to JICF. Of particular note is that as θ continually increases from windward to leeward injection, entrainment continually increases, with near lateral injection (near 90°) having entrainment comparable to the baseline JICF. The most suppression of entrainment occurs in case I15, with the effectiveness about 0.75, and the most enhancement of entrainment occurs in case I165, with the effectiveness about 1.3, at the near field station x/rd = 0.5. Finally, our preliminary comparison but under slightly different conditions of the present result at r of 12 and our previous result at r of 4 (Chaikasetsin *et al*. [3]) suggests that JICF at higher r has higher entrainment while the use of azimuthal control jets with JICF at lower r is more effective.

***Keywords**:* Jet in crossflow, entrainment, flow control, azimuthal control jets, probability structure

1. Introduction

Jet in crossflow (JICF) is a flow in which a jet fluid is injected normally from an orifice into an incoming stream of crossflow fluid. The jet interacts with, and bends into the direction of, the crossflow resulting in important characteristics of JICF such as jet structures, trajectory, entrainment, and mixing. JICF and its characteristics are pertinent in engineering applications such as dilution jets in gas turbine combustors (entrainment), dispersion of pollutants from smoke stacks (entrainment, trajectory), and film cooling on gas turbine blades (trajectory, spread). In order to improve the effectiveness of the use of JICF in these applications, researches have been conducted to investigate both the jet structures and characteristics as well as to find a means to manipulate and control these characteristics.

Regarding the jet structures, Fric and Roshko [4] have identified four main vortical structures in JICF, including a counter-rotating vortex pair (CVP). Smith and Mungal [5] found that while CVP is the main mechanism for entrainment in the far field, it does not render mixing enhancement over a free jet; instead, it is the formation of the CVP in the near field that results in mixing enhancement over a free jet. Yuan *et al*. [6] suggested that the CVP is developed from skewed mixing layers at the lateral edges of the jet. Yuan and Street [7] found that JICF entrainment is related to its trajectory in the far field by power law.

In order to manipulate and control JICF, many devices and techniques have been proposed and investigated. Examples are the uses of tabs (Liscinsky *et al*. [8]; Zaman and Foss [9]; Bunyajitradulya and Sathapornnanon [10]), swirling jet (Liscinsky *et al*. [8]; Niederhaus *et al*. [11]; Wangjiraniran and Bunyajitradulya [12]; Bunyajitradulya and Sathapornnanon [10]; Yingjaroen *et al*. [13]; Denev *et al*. [14]), and pulsing (Eroglu and Breidenthal [15]; M'Closkey *et al*. [16]). While fixed tabs are simple, they are passive; actuating and moving tabs are readily active, but both fixed and moving tabs have potential complications in fabrication, operation, and maintenance, especially when they need to be subjected to hazardous environment such as hot gases in combustion chambers; swirling can be active, but past studies show that swirl has little effect on entrainment and mixing; pulsing (of the main jet) is readily active, but pulsing as well as swirling generally require large amount of driving energy.

Subsequently, Kornsri *et al.* [17] (see also Bunyajitradulya [18]) developed the azimuthal control jet technique based on the underlying premise that an effective technique to manipulate and control JICF should be based on the stimulation and perturbation of the formation of flow structures at or near the point of inception of the structures, e.g., near the jet exit. As shown in the above works, the technique proves to be effective in manipulating and controlling JICF trajectory. In addition, it uses relatively less driving energy as well as is readily applicable to active control, e.g., changing the positions of injection θ, adjusting the azimuthal control jets to main jet mass flow rate ratio r_m, or pulsing of the control jets. Specifically, it is found that a pair of azimuthal control jets injected steadily at azimuthal positions $\pm\theta$ can be used to effectively control jet trajectories; windward injection ($\theta < 90^o$) lowers the jet trajectory while leeward injection ($\theta > 90^o$) raises the jet trajectory, when compared to JICF. Nonetheless, the above works could not yet determine the effects of the azimuthal control jets on entrainment, at least not directly. Subsequently, Witayaprapakorn and Bunyajitradulya [1] and Witayaprapakorn [2] investigated the effects of the azimuthal control jets on the accumulative volumetric entrainment ratio (E) of JICF directly and found that injecting a pair of control jets steadily at θ = ± 135° (case I135) enhances entrainment over the baseline uncontrolled JICF while injecting at θ = ± 15° (case I15) suppresses entrainment, at least in the near field. It was suggested that the reduction of entrainment in the near field of I15 was most likely due to wall blocking effect discussed by Kornsri *et al*. [17] (see also Bunyajitradulya [18]). Chaikasetsin *et al*. [3] further investigated the effect of the azimuthal control jets to main jet mass flowrate ratio (r_m) on entrainment for case I135 and found that the jet entrainment increases quite drastically as r_m is increased from 2% to 4%, upto about 60% when compared to either JICF or case r_m = 2% at x/rd = 1.5.

Up to the present, our past researches on the effectiveness of the use of azimuthal control jets for manipulating and controlling JICF structures, trajectory, and entrainment have been focusing mainly on JICF with relatively low effective velocity ratio r of 4 while their effects on JICF with higher r remain unexplored. In addition, as suggested by Smith and Mungal [5], JICF with r less than or equal to 5 is affected by the presence of the wall (wall effect) and most likely belongs to different flow regime than JICF with higher r, where wall effect was suggested to be less prominent. Similar effect of wall blocking of entrainment was also suggested by Denev *et al*. [14] and Kornsri *et al.* [17]. Therefore, the objective of this study is to investigate the effects of azimuthal positions θ of the azimuthal control jets on the accumulative volumetric entrainment ratio E of a jet in crossflow at the higher effective velocity ratio r of 12.

2. Experimental Technique for the Determination of Entrainment

The principle of the experimental technique of using Stereoscopic Particle Image Velocimetry (SPIV) with jet fluid only – and not the crossflow fluid – seeding scheme to determine entrainment directly is described in Witayaprapakorn and Bunyajitradulya [1] and Chaikasetsin *et al*. [3]. We briefly summarize it here.

The time-mean accumulative volumetric entrainment ratio E at any streamwise cross plane x is defined as the ratio of the time-mean jet-fluid mixture volume flowrate through the cross plane at x, $Q_j(x)$, and the initial jet volume flowrate at the jet exit, Q_0,

$$E = \frac{Q_j(x)}{Q_0}. \quad (1)$$

If the azimuthal control jets are used, Q_0 is the sum of the volume flowrates from both the main jet and the control jets. The time-mean jet-fluid mixture volume flowrate $Q_j(x)$ can in turn be found from

$$Q_j(x) = \frac{1}{T}\int_0^T Q_j(x,t)dt = \frac{1}{T}\int_0^T \left(\int_{A_j(x,t)} V_x(\vec{x},t)dA \right) dt, \quad (2)$$

where $Q_j(x,t)$ is the instantaneous jet-fluid mixture volume flowrate, $V_x(\vec{x},t)$ is the instantaneous streamwise velocity field, $A_j(x,t)$ is the instantaneous jet-fluid mixture cross section – excluding the surrounding pure crossflow region, $\vec{x}$ is spatial position vector, x is streamwise coordinate in the direction of the crossflow, and t is time.

Due to the unsteady and random nature of turbulent jet, the instantaneous jet-fluid mixture cross section $A_j(x,t)$ is also a function of time t. This results in some difficulty in determining the time-mean jet-fluid mixture volume flowrate $Q_j(x)$ and consequently the time-mean entrainment ratio E since the time-mean integral and the surface integral in Eq. (2) cannot be interchanged. If forced to interchange,

$$Q_j(x) = \int_{A_j^*(x)} V_x(\vec{x})dA\,, \qquad (3)$$

where $V_x(\vec{x}\,)$ is the time-mean streamwise velocity field, some less than well-defined time-mean jet-fluid mixture cross section $A_j^*(x)$ must be determined from some other conditions.

Due to these difficulties and in order to give some indication of entrainment, some of the past works used indirect indicators such as decay and spread rates of selected mean quantities such as mean temperature and mean passive scalar concentration and mostly only in the center plane (see, e.g., Kamotani and Greber [19], Smith and Mungal [5], Wangjiranirun and Bunyajitradulya [12]). These indicators have drawbacks in that they are *indirect*: they are not a measure of volumetric entrainment ratio E directly, and/or they are *incomplete*: usually data only in the limited region, e.g., in the center plane, which do not take into account the distribution of the quantity over the cross plane, are used.

On the other hand, in those works, notably e.g., Yuan and Street [7], that attempted to determine the volumetric entrainment ratio E more directly according to Eq. (1), due to the unavailability of the *instantaneous* field data, had to start off with the *mean* fields such as mean passive scalar concentration and velocity fields. As a result, they are forced to use Eq. (3) and consequently to set *arbitrary* threshold value – with some degree of arbitrariness – for the mean scalar concentration in order to mark the jet edge and in order to determine $A_j^*(x)$, and subsequently $Q_j(x)$ and E.

In order to overcome these past difficulties and to determine the time-mean entrainment E directly, we can see from Eq. (2) that in order to be able to determine the time-mean jet-fluid mixture volume flowrate $Q_j(x)$ accurately, 1) the jet-fluid mixture cross section $A_j(x,t)$ must be instantaneously and clearly identified and differentiated from the surrounding pure crossflow region, and 2) the instantaneous velocity component perpendicular to the cross plane, i.e., V_x, must be measured instantaneously over a cross plane, at all times. This has led Witayaprapakorn and Bunyajitradulya [1], Chaikasetsin *et al.* [3], and Wongthongsiri and Bunyajitradulya [20] to the use of SPIV in which only the jet fluid – and not the crossflow fluid – is seeded with PIV tracer particles. The PIV tracer particles then act as both jet-fluid mixture marker and PIV tracers to measure the jet velocity field. As a result, the SPIV registers only velocity vectors from the jet-fluid mixture region (i.e., the region with some PIV tracer particles, or with some main jet fluid) and registers none from the surrounding pure crossflow region (i.e., the region with no PIV tracer particles, or no main jet fluid). In order to have visual comparison, Fig. 1 shows the two seeding schemes. Figure 1(a) shows the typical case in which both jet and crossflow fluids are seeded, which is not employed in the present work. In this case, the instantaneous jet-fluid mixture region cannot be clearly and instantaneously identified and differentiated from the surrounding pure crossflow region; therefore the instantaneous volume flowrate of the jet-fluid mixture cannot readily be determined. On the other hand, Fig. 1(b) shows the seeding scheme employed in this work – the jet-fluid only seeding scheme. In contrast, in this case the instantaneous jet-fluid mixture cross section can be clearly and instantaneously identified and differentiated from the surrounding pure crossflow region. Consequently, the instantaneous jet-fluid mixture volume flowrate $Q_j(x,t)$, the time-mean jet-fluid mixture volume

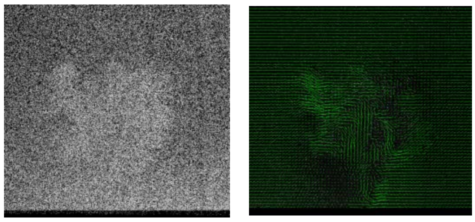

(a) Both jet and crossflow fluids seeding scheme.

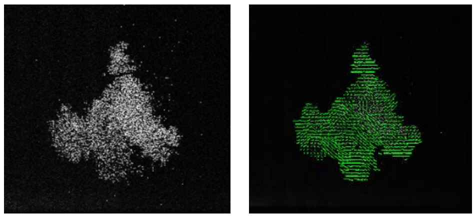

(b) Jet fluid only seeding scheme.

Fig. 1. Comparison of the instantaneous particle images (left) and the processed instantaneous vector fields (right) between
(a) both jet and crossflow fluids seeding scheme, and
(b) jet-fluid only seeding scheme.

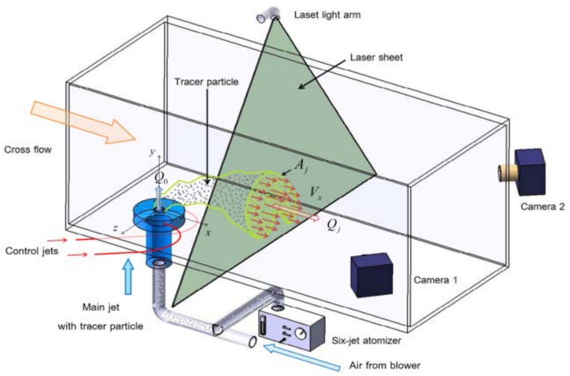

Fig. 2. Schematic diagram of the experimental setup (Chaikasetsin *et al*. [3]).

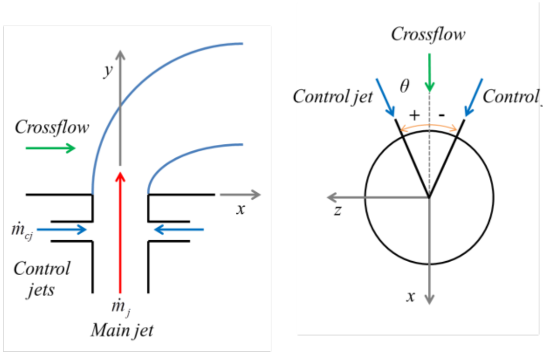

Fig. 3. Main jet and control jets configuration (Chaikasetsin *et al*. [3]).

flowrate $Q_j(x)$, and subsequently the time-mean accumulative volumetric entrainment ratio E can be determined directly from Eqs. (2) and (1). For further details in this regard, the reader is referred to Witayaprapakorn and Bunyajitradulya [1], and Chaikasetsin *et al*. [3].

3. Experimental Setup

3.1. Experimental apparatus

Figure 2 shows the schematic diagram of the experimental setup. Except for the main jet and control jet assembly, which is newly replaced, the experimental setup is almost identical to Witayaprapakorn and Bunyajitradulya [1], and Chaikasetsin *et al*. [3]. Briefly, the crossflow is generated in the same 50x50 cm^2 wind tunnel test section. However, the main jet and control jet assembly is replaced with a main jet with inner diameter (d) of 12.57 mm and a series of azimuthal control jets with inner diameter of 0.5 mm. The azimuthal control jets are located 3 mm below the main jet exit plane and they are uniformly spaced at 15 degrees apart. The configuration for the main and control jets assembly is shown in Fig. 3.

3.2. Stereoscopic Particle Image Velocimetry

The planar measurement of the velocity field vector (V_x, V_y, V_z) at each cross plane is measured with TSI™ Stereoscopic Particle Image Velocimetry (SPIV) system. The SPIV laser is New Wave Research Nd:YAG laser (model Solo 200XT) with 200 mJ nominal energy per pulse at 532 nm wavelength. The laser is guided through a light arm, formed into a sheet by light sheet optics, and illuminates the PIV tracer particles in the test section. The tracer particles are 5% by volume glycerol solution, seeded into the pipe far upstream from the main jet exit to ensure particle uniformity before the jet exit by a TSI™ six-jet atomizer. Two PowerView Plus 11MP CCD cameras with Nikkor 50 mm f/1.8D lenses are used, each to capture 1,000 image pairs of the particles, which results in 1,000 instantaneous three-dimensional velocity field snapshots. The CCD pixel format is 4,008x2,672 pixel^2 and the pixel size is 9x9 μm^2. The laser and cameras are synchronized by a synchronizer. The particle images are analyzed and the instantaneous velocity field snapshots are rendered by TSI™ Insight 4G program. The instantaneous velocity fields of 1,000 instants are then further analyzed by in-house MATLAB program.

The three-dimensional velocity field snapshots are collected at the rate of 1.04 Hz. The spatial resolution of the velocity fields ranges between 2.28 mm x 2.28 mm to 2.95 mm x 2.95 mm over the range of x/rd stations collected. In addition, there are approximately more than 4,700 vectors at x/rd = 0.5 and more than 8,300 vectors at x/rd = 1.5 in the time-mean velocity field results.

3.3. Experimental scope and condition

The experiment is conducted for the baseline JICF at the effective velocity ratio r of 12.0 ± 0.3. Note that r is defined by $r = \sqrt{\rho_j u_j^2 / \rho_{cf} u_{cf}^2}$, where ρ is density, u is velocity, and the subscripts j and cf refer to the jet and the crossflow, respectively. For the present experiment, ρ_j and ρ_{cf} are equal at atmospheric density; u_j is the area-averaged jet velocity at the main jet exit (measured when the crossflow and the control jets are off), which is measured to be 49.2 m/s; while u_{cf} is the uniform crossflow velocity, which is measured to be 4.0 m/s. The crossflow Reynolds number ($\mathrm{Re}_{cf} = u_{cf} d / \nu_{cf}$, ν is kinematic viscosity) is 3,100; the jet initial velocity profile is fully-developed turbulent pipe flow. The incoming crossflow boundary layer is laminar, with relative thickness measured at x/d = -2 of $\delta_{95\%}/d$ = 0.64.

When azimuthal control jets are deployed, a pair of azimuthal control jets is injected radially and steadily at the azimuthal positions θ = ±15° (I15), ±45° (I145), ±75° (I75), ±105° (I105), ±135° (I135), and ±165° (I165) and at the azimuthal control jets to

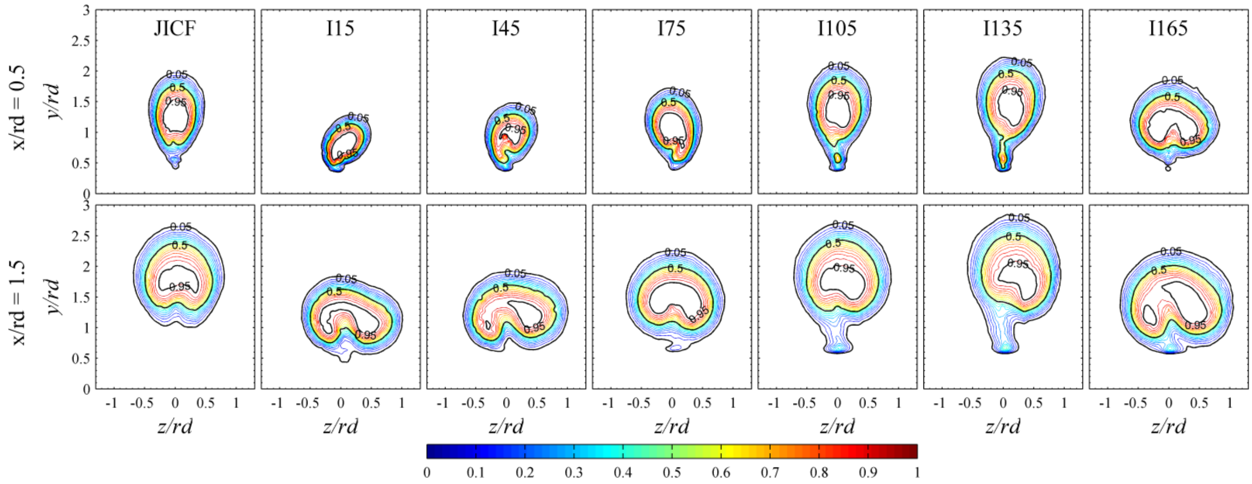

Fig. 4. Effect of the azimuthal control jets position θ on the probability of finding jet fluid at a point, ϕ_{ij}. Note that, while considered as part of the jet-fluid mixture cross section, the jet region in the range $0 < \phi_{ij} < 0.05$ is not shown in the figures. Contour line resolution is 0.05.

main jet mass flowrate ratio (r_m) of 4%. Note that r_m is defined as $r_m = \dot{m}_{cj} / \dot{m}_j$, where $\dot{m}_{cj}$ is the total mass flowrate of the (two) control jets and $\dot{m}_j$ is the mass flowrate of the main jet. Measurements are made at four downstream cross planes located at x/rd = 0.5, 0.75, 1.0 and 1.5.

4. Results

4.1. Effect of θ on the probability of finding jet fluid at a point, ϕ_{ij}

The use of SPIV with the jet-fluid only seeding scheme does not only allow use to determine the jet volumetric entrainment ratio more directly, it also allows us to determine the probability of finding jet fluid (or jet-fluid mixture) at a spatial point ϕ_{ij}. The probability of finding jet fluid at a spatial point ϕ_{ij} is defined by

$$\phi_{ij} = N_{v,ij} / N, \qquad (4)$$

where $N_{v,ij}$ is the number of instants at which jet fluid (i.e., tracer particles) is found at spatial point (i, j) as marked by non-zero velocity vector registered by the SPIV, and N is the total number of data-acquisition instants. In addition, the probability of finding jet fluid at a spatial point ϕ_{ij} is a complement to the probability of finding pure crossflow fluid at a spatial point $\phi_{cf,ij}$, i.e., $\phi_{ij} + \phi_{cf,ij} = 1$.

Figure 4 shows the effect of the azimuthal control jets position θ on the probability of finding jet fluid at a point. Due to the jet-fluid only seeding scheme, in general ϕ_{ij} has high value near the jet center, where the probability of finding jet fluid is high; decreases and approaches zero as we approach the jet edge; and becomes zero in the pure crossflow region far away from the jet where no jet fluid can be found at all times.

The results in Fig. 4 shows that overall windward injection ($\theta < 90^o$) of azimuthal control jets causes the jet to penetrate less into the crossflow and modifies the jet probability structure considerably when compared to JICF. On the other hand, leeward injection ($\theta > 90^o$) of azimuthal control jets generally has the opposite effects. That is, it typically causes the jet to penetrate deeper into the crossflow (except the extreme case of I165) and modifies the jet structure to a lesser extent when compared to JICF. Nonetheless, of particular note is that leeward injection (again except the extreme case of I165) promotes the wake-like structure at the underside of the jet, especially in cases I105 and I135. In other words, there is relatively high probability of finding jet fluid in the wake-like structure at the underside of the jet in these cases.

The present results of the effects of azimuthal control jets position θ on the jet penetration and trajectory, and on the jet structure are in general consistent with the results of Kornsri *et al.* [17] on the jet center plane $w = \sqrt{V_x^2 + V_y^2}$ velocity trajectory and the corresponding jet velocity structure, and with the results of the effects of tab disturbance on the mean temperature structure of Bunyajitradulya and Sathapornnanon [10]. The effects of azimuthal control jets position θ on the jet trajectory will be quantified more clearly in Sec. 4.4.

4.2. Effect of θ on the structure of the normalized time-mean streamwise jet velocity, V_x / u_{cf}

Figure 5 shows the effect of the azimuthal control jets position θ on the structure of the normalized time-mean streamwise jet velocity, V_x / u_{cf}. Naturally,

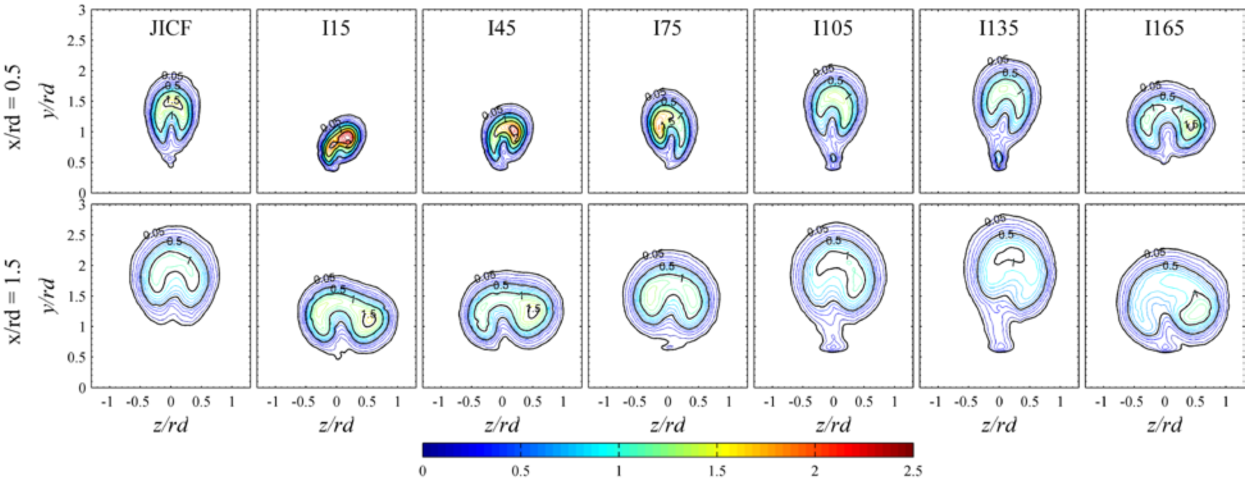

Fig. 5. Effect of the azimuthal control jets position θ on the normalized time-mean streamwise jet velocity, V_x / u_{cf} . Contour line resolution is 0.1.

overall the V_x -structure is similar to the ϕ_{ij} -structure in the sense and to the extent that we can have non-zero value of the time-mean streamwise jet velocity only at points where we can find jet fluid ($\phi_{ij} > 0$). However, the distributions of the two quantities naturally need not be the same. This is also true with the ϕ_{ij} -structure and the structures of other jet field properties such as velocity and vorticity. Also, for convenience, we refer to the distributions of the probability of finding jet fluid at a point ϕ_{ij} and of the normalized time-mean streamwise jet velocity, V_x / u_{cf} , simply as the ϕ_{ij} -structure and the V_x -structure, respectively.

Of particular note is that windward injection tends to increase, while leeward injection to decrease, the maximum value of the time-mean streamwise jet velocity to various degrees depending upon θ, when compared to JICF. In addition, as θ increases azimuthally from the extreme windward side (I15) to the extreme leeward side (I165), the degree of influencing the maximum value of streamwise jet velocity changes from promoting to suppressing; in other words, from accelerating to decelerating the jet, at least locally, when compared to JICF - with the possible exception at I165 itself. In addition, the wake-like structure in cases of leeward injection I105 and I135 are still prominent. As the jet develops downstream, the V_x -structure grows in size and decays in maximum value in all cases; both are the indirect indicators of increasing entrainment as the jet develops downstream.

4.3. Effect of θ on the structure of the normalized time-mean streamwise jet vorticity, $\omega_x d / u_{cf}$

Figure 6 shows the effect of the azimuthal control jets position θ on the structure of the normalized time-

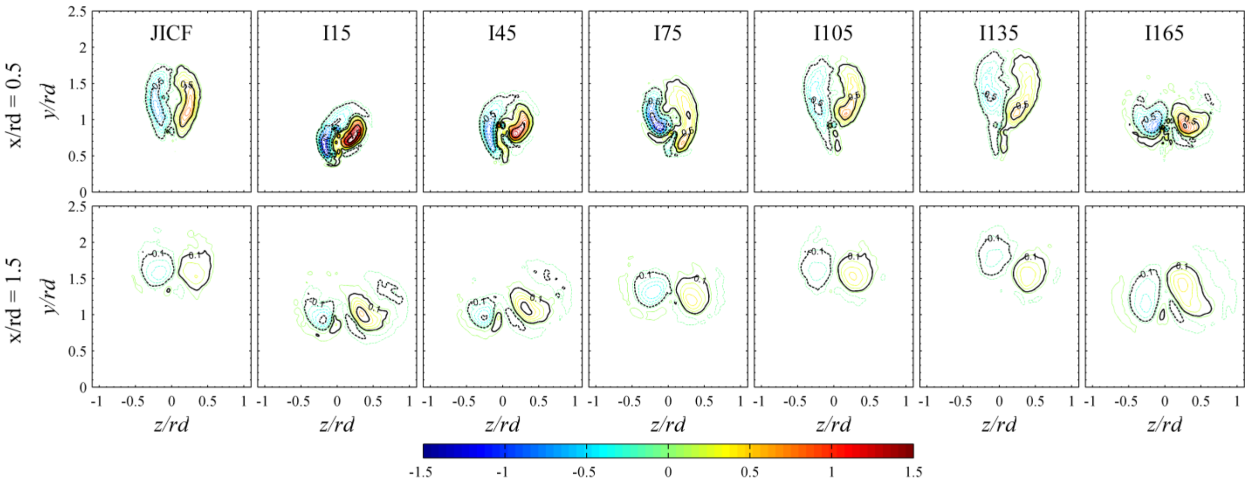

Fig. 6. Effect of the azimuthal control jets position θ on the normalized time-mean streamwise jet vorticity, $\omega_x d / u_{cf}$. Contour line resolution is 0.1.

mean streamwise jet vorticity, $\omega_x d / u_{cf}$. Similarity between the effects of θ on the maximum value of the streamwise jet velocity in Fig. 5 and on the maximum value of the magnitude of the streamwise jet vorticity here can be observed. Specifically, especially in the near field, windward injection tends to increase, while leeward injection to decrease, the maximum value of the magnitude of the streamwise jet vorticity, when compared to JICF, except perhaps case I165. In other words, windward injection tends to promote while leeward injection to suppress angular motion of the vortical structure – at least locally. In addition, as θ increases azimuthally from the extreme windward side (I15) to the extreme leeward side (I165), the degree of influencing the maximum value of the magnitude of the streamwise jet vorticity changes from promoting to suppressing, when compared to JICF, also with the possible exception at I165 itself. As the jet develops downstream, the maximum value of the magnitude of the streamwise jet vorticity decreases in all cases.

4.4. Effect of θ on the jet trajectories

The trajectory of a jet property X (i.e., a property that is associated with jet-fluid mixture, excluding the contribution from pure crossflow fluid) is defined here as the locus of the center of mass of the absolute value, or the magnitude, of the time-mean jet property X in the transverse direction, $y_{CM,|X|}$,

$$y_{CM,|X|} = \frac{\int_{A_j} y|X|dA}{\int_{A_j} |X|dA} . \tag{5}$$

Figure 7(a) shows the effects of the azimuthal control jets position θ on the streamwise jet velocity trajectory $y_{CM,|V_x|}$ and Fig. 7(b) on the streamwise jet vorticity trajectory $y_{CM,|\omega_x|}$, together with the power law fits:

$$(y/rd) = a(x/rd)^b . \tag{6}$$

The results show that the effects of θ on both trajectories are similar. That is, except case I165, windward injection lowers the jet trajectories; while leeward injection raises the jet trajectories, when compared to JICF. In addition, as the azimuthal control jets position θ continually increases from the extreme windward (I15) to leeward (I135), the jet trajectories become higher, with the trajectory of I105 being comparable to JICF. Exception is the case I165 in which as θ increases from I135 to I165, the jet trajectories instead become lower and comparable to case I75. Furthermore, the power-law fits describe both velocity and vorticity trajectories fairly well. These results are consistent with those of Kornsri *et al.* [17] on the center plane $w = \sqrt{V_x^2 + V_y^2}$ velocity trajectory. In addition, the results show that the vorticity trajectory $y_{CM,|\omega_x|}$ always lies below the velocity trajectory $y_{CM,|V_x|}$ for all cases, consistent with the results of Wongthongsiri and Bunyajitradulya [20].

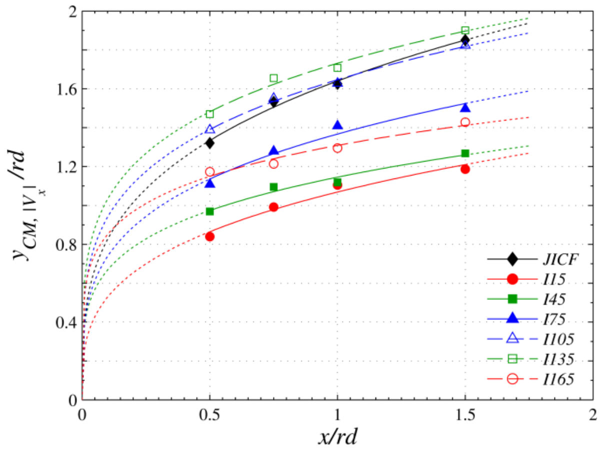

(a) Streamwise jet velocity trajectory, $y_{CM,|V_x|}$.

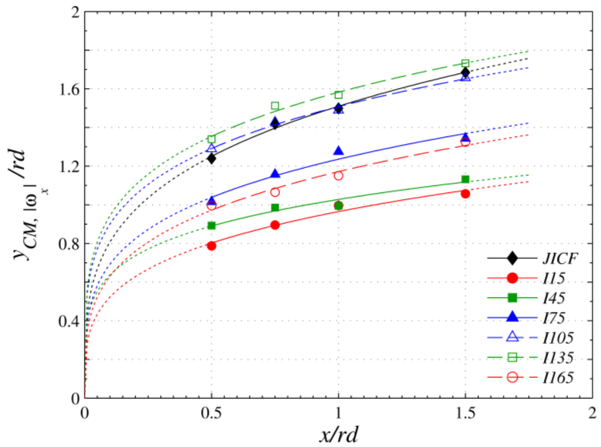

(b) Streamwise jet vorticity trajectory, $y_{CM,|\omega_x|}$.

Fig. 7. Effects of the azimuthal control jets position θ on the jet trajectories.

4.5. Effect of θ on entrainment and effectiveness

Figure 8(a) shows the effects of the azimuthal control jets position θ on the time-mean accumulative volumetric entrainment ratio E for all cases together with the power law fits:

$$E = 1 + a(x/rd)^b . \tag{7}$$

The result, especially in the near field, shows that overall windward injection suppresses entrainment while leeward injection promotes entrainment, when compared to JICF. In addition, as θ increases from the extreme windward injection (I15) to the extreme leeward injection (I165), entrainment continually increases, with injection near 90° (I75 and extrapolated to I90) having entrainment comparable to the baseline JICF. Also, the power law fits describe the evolutions of entrainment only fairly well.

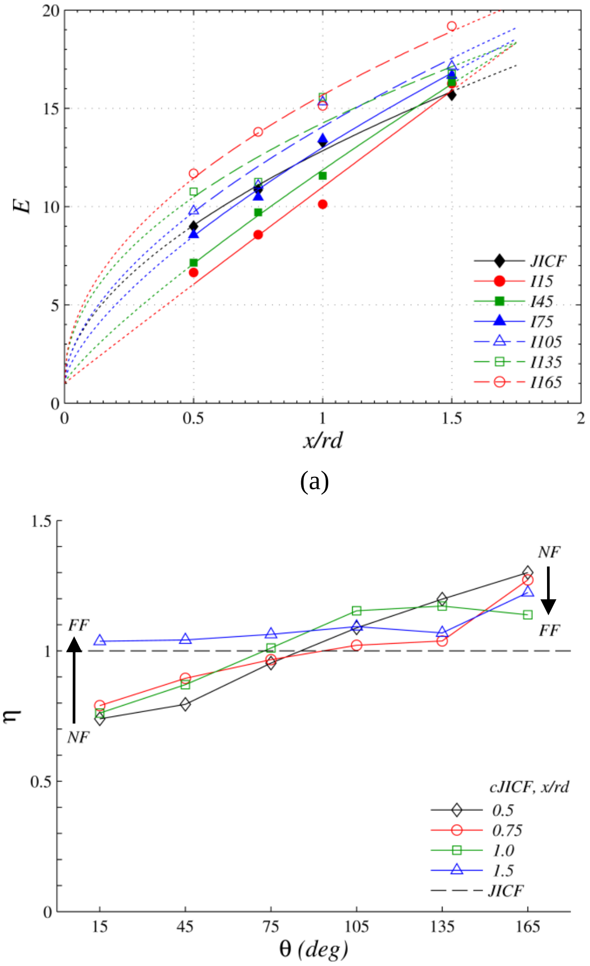

(a)

(b)

Fig. 8. Effect of the azimuthal control jets position θ on
(a) accumulative volumetric entrainment ratio E, and
(b) effectiveness η.

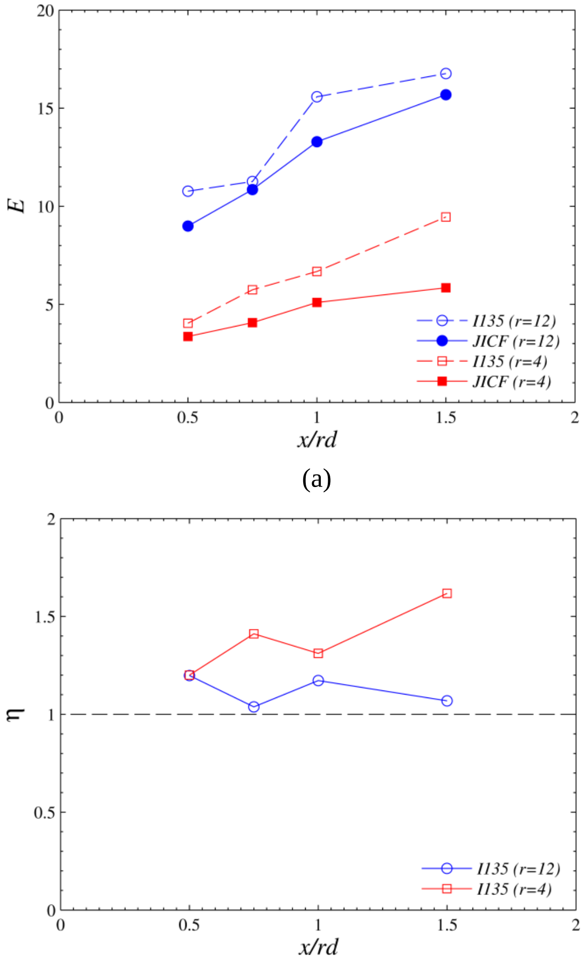

(a)

(b)

Fig. 9. Comparison of entrainment and effectiveness between the present work at r =12 (blue) and those of Chaikasetsin *et al.* [1] at r = 4 (red):
(a) accumulative volumetric entrainment ratio E, and
(b) effectiveness η.

The effect of the azimuthal control jets position $y_{CW,j}$ on promoting/suppressing entrainment when compared to JICF is more clearly seen when we consider the effectiveness of the use of the azimuthal control jets, η, defined as the ratio between the entrainment ratio of the controlled case (E_{cJICF}) to the entrainment ratio of the uncontrolled JICF (E_{JICF}),

$$\eta = \frac{E_{cJICF}}{E_{JICF}}. \tag{8}$$

Figure 8(b) shows the effectiveness for all cases and planes. Recognizing that these results are within the limited scope of downstream stations investigated, the followings can be observed.

1) Especially in the near field, windward injection suppresses entrainment, with case I15 having the lowest entrainment and lower than JICF. On the contrary, leeward injection promotes entrainment, with case I165 having the highest entrainment and higher than JICF.
2) With a few exceptions, as $y_{CW,j}$ increases azimuthally from windward to leeward, the effectiveness η increases, with near lateral injection (I75 and extrapolated to I90) having comparable entrainment to the baseline JICF, i.e., $\eta \cong 1$.
3) For the extreme windward (near and towards I15) or leeward (near and towards I165) injections, the effect of the azimuthal control jets position θ on effectiveness and entrainment is more pronounced in the near field.
4) Within the scope of parameters experimented, the most enhancement of entrainment occurs in I165 at x/rd = 0.5 with η = 1.3, and the most

suppression of entrainment occurs in I15 at x/rd = 0.5 with η = 0.75.

5. Discussion on the entrainment and the effectiveness for JICF with different r

In order to gauge the differences in entrainment and effectiveness of the use of the azimuthal control jets with JICF of different effective velocity ratio r, we compare the present cJICF case of I135, $r_m = 4\%$ at r of 12 to that of Chaikasetsin *et al.* [3] at the same injection case of I135, $r_m = 4\%$ but at lower r of 4. However, recognize first that besides r the two works are not quite at the same condition. Of particular notes are the crossflow Reynolds number of the present work is lower at 3,100 as opposed to 5,600 of Chaikasetsin *et al.* [3]; and the normalized crossflow boundary layer thicknesses δ/d are also different. With this, Fig. 9(a) shows that the entrainment of JICF at higher r of 12 is considerably higher than the entrainment of JICF at lower r of 4. In addition, when azimuthal control jets are applied at I135, both works show increase in entrainment. However, when we consider the effectiveness in Fig. 9(b), we find that overall the case of lower r of 4 generally has higher effectiveness than the case of higher r of 12. Whether the difference in effectiveness can be mainly accounted for by the difference in r alone is still not yet conclusive.

Finally, it should be strongly cautioned that the above comparisons for entrainment and effectiveness for JICF with different r in Fig. 9 are based on the downstream distance in rd-scale. However, the above conclusions are still valid when we compare them based on the downstream distance in d-scale, at least within the limited scope of downstream distance investigated.

6. Conclusions

The effects of the azimuthal position θ of the azimuthal control jets on the structure and entrainment of a jet in crossflow at the effective velocity ratio of 12 are investigated. Stereoscopic Particle Image Velocimetry (SPIV) together with the jet-fluid only seeding scheme is employed in order to determine entrainment. The velocity field is measured at the cross planes x/rd = 0.5, 0.75, 1.0, and 1.5.

The results show that the azimuthal control jets position θ affects the jet structure, trajectories, entrainment, and effectiveness. Typically, with a few exceptions, windward injection ($\theta < 90^o$) significantly modifies the jet probability, velocity, and vorticity structures; enhances maximum streamwise velocity and (magnitude of) vorticity; lowers the jet trajectories; and suppresses entrainment, making the effectiveness less than one, when compared to JICF. On the other hand, leeward injection ($\theta > 90^o$) typically has the opposite effects; namely, modifies the jet structures relatively less – except for the appearance of the wake-like region at the underside of the jet; diminishes maximum streamwise velocity and (magnitude of) vorticity; raises the jet trajectories (except case I165), and promotes entrainment, making the effectiveness more than one, when compared to JICF. In addition, as θ continually increases from the extreme windward side (I15) to the extreme leeward side (I165) – with exceptions at I165 itself – the degree of influencing these characteristics continually changes. Of particular notes are the followings. As θ continually increases from the extreme windward side (I15) to the extreme leeward side (I165):

1. The degree of influencing the maximum value of streamwise jet velocity and (magnituder of) vorticity changes from promoting to suppressing, when compared to JICF - with the possible exception at I165 itself; in other words, from accelerating to decelerating both linear and angular motions of the jet in the streamwise direction – at least locally.
2. The jet streamwise velocity and vorticity trajectories become higher, with the trajectory of I105 being comparable to JICF. Exception is the case I165 in which as θ increases from I135 to I165, the jet trajectories instead become lower and comparable to case I75.
3. The degree of influencing the jet entrainment changes from suppressing to promoting, with injection near 90º (I75 and extrapolated to I90) having entrainment comparable to the baseline JICF. As a result, the degree of influencing the effectiveness of the use of azimuthal control jets in promoting entrainment changes from less effective to more effective accordingly.

Furthermore, the followings are observed:

4. The effect of the azimuthal control jets position on effectiveness is more pronounced in the near field, especially in the extreme windward (near and towards I15) and leeward (near and towards I165) injections.
5. Within the scope of parameters experimented, the most enhancement of entrainment occurs in I165 with η = 1.3 and the most suppression of entrainment occurs in I15 with η = 0.75, both at x/rd = 0.5.
6. By preliminarily comparing the present result of the baseline cases of JICF at r of 12 and our previous result at r of 4, and of cJICF at the same injection angle $\pm 135^{\circ}$ and mass flowrate ratio r_m of 4% (Chaikasetsin *et al.* [3]), our comparison suggests that JICF at higher r has higher entrainment while the use of azimuthal control jets with JICF at lower r is more effective. However, due to the difference in conditions, this is not yet conclusive.

7. Acknowledgements

The Thai Government Research Funds for the fiscal years 2556: Contract Nos. GRB_APS_21_56_21_04 and fiscal years 2557: Contract No. GRB_APS_23_57_21_01, and The Thailand Research Fund and The Commission on Higher Education under the Grant No. RMU5080047, are gratefully acknowledged. We would like to express our appreciation for their useful suggestions and assistances to Mr. Settasit Chaikasetsin, Mr. Kittikun Wongthongsiri, Mr. Suphak Dawyok, and Mr. Apichet Srimekharat; for their assistances and cooperations to Mr. Anand Kulpiyavaja, Mr. Apiwat Chaninwongsiri, Mr. Phattarapol Suppamongkol, Miss Kwanmon Sornphrom, and Miss Minthanon Chairat.

8. References

[1] Witayaprapakorn, T. and Bunyajitradulya, A. (2013). Effects of azimuthal control jets on structure and entrainment of a jet in crossflow, paper presented in *the Twenty-Seventh Conference of the Mechanical Engineering Network of Thailand*, Chonburi, Thailand.

[2] Witayaprapakorn, T. (2013). Effects of azimuthal control jets on the entrainment of a jet in crossflow, Master thesis, Department of Mechanical Engineering, Faculty of Engineering, Chulalongkorn University.

[3] Chaikasetsin, S., Sushewakhul, T., Panusittikorn, P. and Bunyajitradulya, A. (2014). Effects of azimuthal control jets to main jet mass flowrate ratio on the entrainment of a jet in crossflow, paper presented in *the 5th TSME International Conference on Mechanical Engineering*, Chiang Mai, Thailand.

[4] Fric, T.F., Roshko, A. (1994). Vortical structure in the wake of a transverse jet, *J. Fluid Mech.*, vol. 279, pp. 1-47.

[5] Smith, S.H. and Mungal, M.G. (1998). Mixing, structure and scaling of the jet in crossflow, *J. Fluid Mech.*, vol. 357, pp. 83-122.

[6] Yuan, L.L., Street, R.L., and Ferziger, J.H. (1999). Large-eddy simulation of a round jet in crossflow, *J. Fluid Mech.*, vol. 379, pp. 71-104.

[7] Yuan, L.L. and Street, R.L. (1998). Trajectory and entrainment of a round jet in crossflow, *Phys. Fluids*, vol. 10, no. 9, pp. 2323-2335.

[8] Liscinsky, D.S., True, B., and Holdeman, J.D. (1995). Effects of initial conditions on a single jet in crossflow, *AIAA J.*, paper no. 95-2998.

[9] Zaman, K.B.M.Q. and Foss, J.K. (1997). The effect of vortex generators on a jet in a crossflow, *Phys. Fluids*, vol. 9, pp. 106-114.

[10] Bunyajitradulya, A. and Sathapornnanon, S. (2005). Sensitivity to tab disturbance of the mean flow structure of nonswirling jet and swirling jet in crossflow, *Phys. Fluids*, 17, 045102.

[11] Niederhaus, C.E., Champagne, F.H., and Jacobs, J.W. (1997). Scalar transport in a swirling transverse jet, *AIAA J.*, vol. 35, no. 11, pp. 1697-1704.

[12] Wangjiraniran, W. and Bunyajitradulya, A. (2001). Temperature distribution in non-zero circulation swirling jet in crossflow, paper presented in *the Fifteenth Conference of The Mechanical Engineering Network of Thailand*, Bangkok, Thailand.

[13] Yingjaroen, T., Pimpin, A., and Bunyajitradulya, A. (2006), Evolution of mixing regions in jet and swirling jet in crossflow: An experimental study, paper presented in *the Twentieth Conference of the Mechanical Engineering Network of Thailand*, Nakhon Ratchasima, Thailand.

[14] Denev, J.A., Fröhlich, J., and Bockhorn, H., (2009). Large eddy simulation of a swirling transverse jet into a crossflow with investigation of scalar transport, *Phys. Fluids*, 21, 015101.

[15] Eroglu, A. and Breidenthal, R.E. (2001). Structure, penetration, and mixing of pulsed jets in crossflow, *AIAA J.*, vol. 39, no. 3, pp. 417-423.

[16] M'Closkey, R.T., King, J.M., Cortelezzi, L., and Karagozian, A.R. (2002). The actively controlled jet in crossflow, *J. Fluid Mech.*, vol. 452, pp. 325-335.

[17] Kornsri, P., Pimpin, A., and Bunyajitradulya, A. (2009). A scheme for the manipulation and control of a jet in crossflow: The use of azimuthal control jets, paper presented in *the Twenty-Third Conference of the Mechanical Engineering Network of Thailand*, Chiang Mai, Thailand.

[18] Bunyajitradulya, A. (2011). Manipulation and control of the entrainment of a jet in crossflow, TRF RMU5080047 Research Project Report, Thailand Research Fund (TRF).

[19] Kamotani, Y. and Greber, I. (1972). Experiments on a turbulent jet in a cross flow, *AIAA J.*, vol. 10, no. 11, pp. 1425-1429.

[20] Wongthongsiri, K., and Bunyajitradulya, A. (2014). Effects of crossflow Reynolds number on structures and entrainment of a jet in crossflow, paper presented in *the 5th TSME International Conference on Mechanical Engineering*, Chiang Mai, Thailand.